

## Proposed Formulation Using ANSYS for Estimation Axially Strength of Steel Tubes Columns Filled with Concrete

Marwah S. Abdul Gbabar 

Building and Construction Engineering Department, University of Technology/Baghdad.

Email” marwasafa85@yahoo.com

Received on:7/3/2016 & Accepted on:22/6/2016

### ABSTRACT

In this paper, concrete filled steel tubes columns (CFT) are investigated by using finite element program ANSYS 15.0. Analysis are done for four different shapes of columns (circular, square, hexagonal and octagonal). Results of analytical solution (for circular and square) were compared with existing experimental data provided by [Alwash et al., 2013]. Comparative results of failure load give 4% difference between experimental and ANSYS 15.0. Also, parametric studies have been carried out to investigate the effect of concrete filled steel tubes columns shapes (for hexagonal and octagonal) on load carrying capacity. Finally, a new formulae for predicting the ultimate strength of CFT is proposed based on experimental data of 148 CFT columns of different cross sections with side length ranging between 200 and 4000 mm. To check the validity of the proposed equation, the loads calculated from the design methods (American Concrete Institute (ACI 318M-14), Eurocode (EC4), New Zealand Standard of concrete structures (NZS) and American Institute of Steel Construction (AISC)) are used to compare with it. The comparison shows least convergence percentage of the proposed equation.

**Keywords:** Short columns, ANSYS, Filled Steel Tubes, Confinement of concrete, Drucker-Prager model.

### INTRODUCTION

Concrete-filled steel tube (CFT), in which the advantages of steel and concrete, has been developed significant improvement in axial capacity without increases in cross-sectional area and provide long spans. Since the steel tube can serve as a form for casting of concrete core, CFT structures possess economical merits in construction. It provides not only an increase in the load carrying capacity due to the confining effect provided by the steel tube but also economy and rapid construction, and thus additional cost saving. Furthermore, occurrence of the local buckling of steel tube is delayed by the restraint of concrete <sup>[1]</sup>.

CFT of different shapes such as circular, rectangular, square, hexagonal, elliptical and any shape can be designed, based on its application. According to the form of concrete core CFT members can be divided into two types: solid and hollow concrete core. Moreover, to improve the behavior of CFT columns, the internal surface of a steel tube can be stiffed by using steel strips, using CFRP on its surface, etc. Also, the structural steel can be encased by reinforced concrete or connected to a reinforced concrete slab including or excluding shear connectors to form beams <sup>[2]</sup>.

The purpose of this research was to study the behavior of composite columns of different shapes of columns circular and square cross-sections by using finite element analysis ANSYS 15.0, and compared these results of load carrying capacity with those reported by [Alwash et al., 2013]. Furthermore, a parametric study of hexagonal and octagonal cross section columns were modeled and compared by ANSYS. At the end of this paper, an empirical equation to calculate the failure load of CFT columns will be proposed.

### Concrete confinement

When concrete is subjected to laterally confining pressure, the uniaxial compressive strength ( $f'_{cc}$ ) and the corresponding strain ( $\epsilon_{cc}$ ), as shown in Figure (1), are much higher than those of unconfined concrete ( $f'_c$ ). The relations between  $f'_{cc}$ ,  $f'_c$  and between  $\epsilon'_{cc}$ ,  $\epsilon'_c$  are approximated by the following equations (Hua et al., 2005 [4]):

$$\left( \begin{matrix} 1 & - \end{matrix} \right) \dots(1)$$

$$\dots(2)$$

Where:

$k_1$  and  $k_2$  were coefficients that are functions of the concrete mix and lateral pressure. The constants  $k_1$  set as 4.1 and  $k_2 = 5 k_1$  based on the studies of (Richart et al., 1928 [5]).

$f_1$  represents the confining pressure around the concrete core calculated from the following empirical equations [6]:

$$- \quad - \quad \text{For } (21.7 \leq D/t \leq 47) \quad \dots(3)$$

$$- \quad - \quad \text{For } (47 < D/t \leq 150) \quad \dots(4)$$

Where:

D is the outer diameter of the circular column.

t is the wall thickness of steel tube.

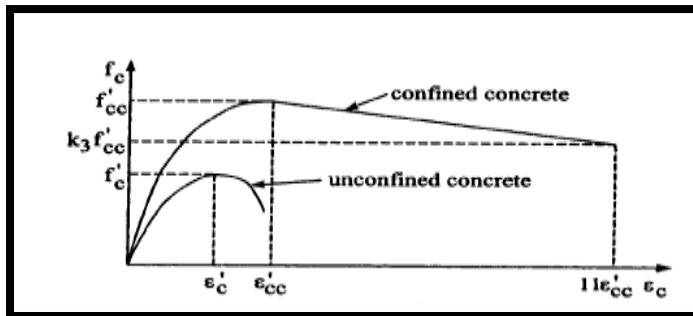


Figure (1): Equivalent uniaxial stress–strain curves for confined and unconfined concrete

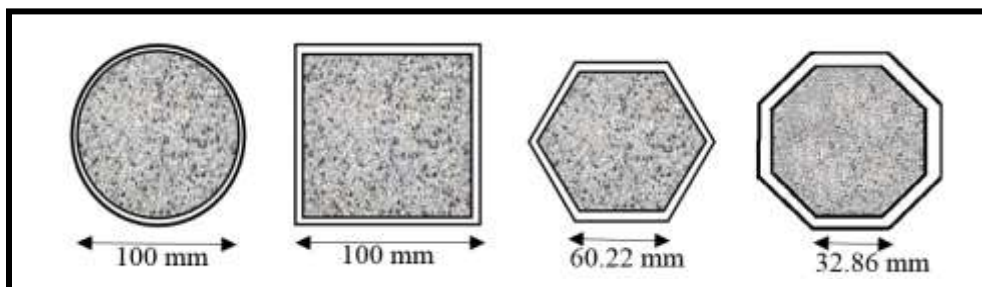
The value of the proportional limit stress is taken as  $0.5(f'_{cc})$  while the initial Young's modulus of confined concrete ( $E_{cc}$ ) is reasonably well calculated using the empirical Eq. (5) given by ACI 318M-14 [7]:

$$\dots(5)$$

**Concrete-filled steel tube Specimen Details modeled by ANSYS**

In order to investigate the behavior of different shapes of concrete filled steel tubes, finite element analysis was conducted by using three dimensional program ANSYS (Version 15) software package. The cross sections of the CFT columns in the numerical analysis are four shapes circular, square, hexagonal and octagonal with 300 mm in length as shown in Figure (2). The columns will be modeled by using ANSYS and results will be compared with the experimentally attained values (for circular and square shapes only) by [Alwash et al., 2013].

The mechanical properties for all the specimens are listed in Table (1) and Table (2) for steel and concrete respectively.



Thickness (mm)	Yield Strength (MPa)	Elastic Modulus (GPa)	Poisson Ratio
2	355	200	0.3

**Figure (2): Cross sections of concrete filled tubes modeled by ANSYS**

Mechanical properties	Compressive strength (MPa)	Elastic Modulus (GPa)	Poisson Ratio
Square models	24.2	22.1	0.2
Circular models	23.5	21.6	0.2

**Table 1: Mechanical properties of steel tube <sup>[3]</sup>**

**Table 2: Mechanical properties of concrete <sup>[3]</sup>**

The dimensions of cross section areas of the two other hollow shapes (Hexagonal and Octagonal) steel tubes were equivalent to the area of steel of circular column with same mechanical properties. The details of steel tubes dimensions modeled by ANSYS are tabulated in Table (3).

**Table (3): Steel tube Specimen details**

Cross Section	Outer dimensions (mm)	Area of hollow Steel tubes (mm <sup>2</sup> )
Square <sup>[3]</sup>	100	784
Circular <sup>[3]</sup>	100	615.44
Hexagonal	60.22	615.44
Octagonal	32.86	615.44

**Concrete material modeling**

To simulate the triaxial behavior of confined concrete with steel tubes with ANSYS, the Drucker-Prager yield criterion has been used. The Drucker-Prager yield criterion (DP) is a pressure-dependent model for determining whether a material has failed or undergone plastic yielding. The yielding surface of the DP criterion may be considered depending on the internal friction angle of the material and its cohesion, and they can be calculated from Equations (6) and (7) respectively <sup>[8]</sup>:

$$\phi = \sin^{-1} \left[ \frac{3}{1+2f'_c/\sqrt{3}} \right] \tag{6}$$

$$c = (f'_c - 5\sqrt{3}) \frac{3-\sin\phi}{6\cos\phi} \tag{7}$$

Where

$f'_c$  in MPa and the cohesion produce from the equation above in MPa,  $\phi$  in degrees.

### Steel material modeling

The stress-strain relation for the steel tube was considered as bilinear-isotropic hardening with slope after yielding.

### Finite element meshing

In the modeling of CFT columns, a properly graded mesh is used for full length of the models. The quadratic element type is used for steel tube and tetrahedral element type for concrete core is adopted. The volume sweep command was used to mesh the steel plate.

### Concrete element type

An eight-node solid element, Solid65, was used to model the concrete. The solid element has eight nodes with three degrees of freedom at each node – translations in the nodal x, y, and z directions. The element is capable of plastic deformation, cracking in three orthogonal directions, and crushing. The geometry and node locations for this element type are shown in Figure (3).

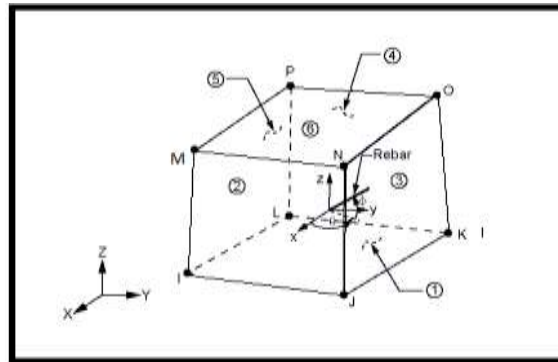


Figure (3): Solid65 geometry (ANSYS)

### Steel element type

An 8-node solid element, Solid185, was used to model the steel. The element is defined by eight nodes having three degrees of freedom at each node: translations in the nodal x, y, and z directions. The element supports plasticity, stress stiffening, large deflection, and large strain capabilities. The geometry and node locations for this element type are shown in Figure (4).

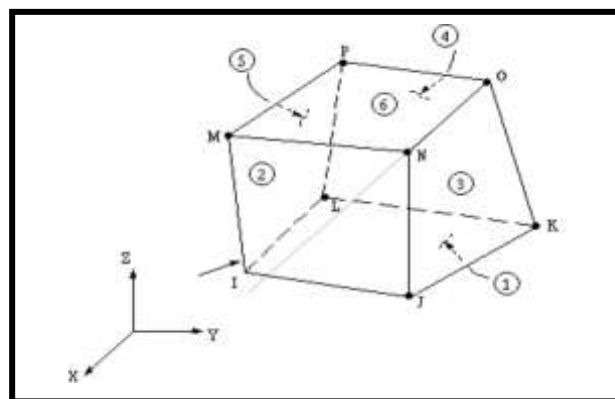


Figure (4): Solid185 geometry (ANSYS)

### Loads procedure and the boundary conditions:

The concrete filled steel tube column was axially loaded by using pressure load option to ensure uniform loading for both concrete and steel. The load applied with time-steps increment equal to 20 kN to ensure correct nonlinear response. The displacements of the bottom end in the

X, Y and Z directions were restrained. Also, the rotations of the bottom end of the columns in the X, Y, and Z directions were set to be zero. On the other hand, the displacement of the top end was considered to be zero for X and Y directions only.

### Nonlinear Analysis

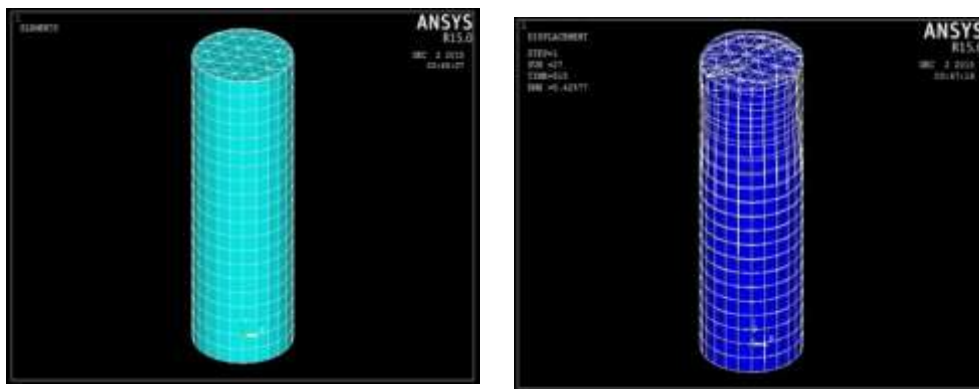
ANSYS uses an iterative process called the Newton-Raphson Method. Newton-Raphson equilibrium iterations provide convergence at the end of each load increment within tolerance limits. If convergence criteria are not satisfied, the out-of-balance load vector is re-evaluated, the stiffness matrix is updated, and a new solution is attained. This iterative procedure continues until the problem converges [9].

### Finite Element Results

Finite element models was analyzed by ANSYS V.15 software in order to validate the results with an existing experimental results made by [3]. Also, a parametric study was carried out with two other shapes (Hexagonal and Octagonal) of CFT to cover a wider range of member cross-sections to examine the structural behavior and failure load.

### Circular CFT

The typical mesh with 1820 elements and the deformed shape of the circular column are shown in Figure (5). The variation of stresses of circular CFT at the ultimate load level illustrate in Figure (6). Also, the load-deflection behavior is shown in Figure (7). Above 100kN, it can be noticed that the Finite element model more stiff than the experimental curve. The finite element solution is in acceptable agreement with the experimental results throughout the entire range of loading. The ratio between experimental and FE failure load is 0.96.



(A) (B)  
Figure (5): (A) Meshed model (B) Deformed shape

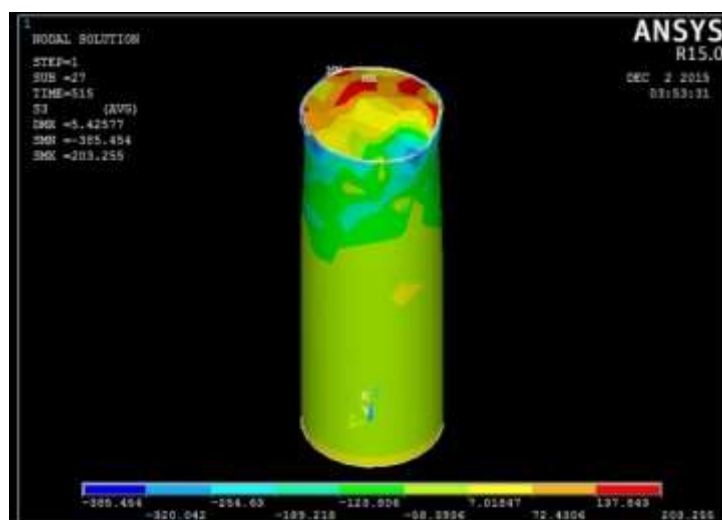


Figure (6): Stresses variation of circular CFT shape

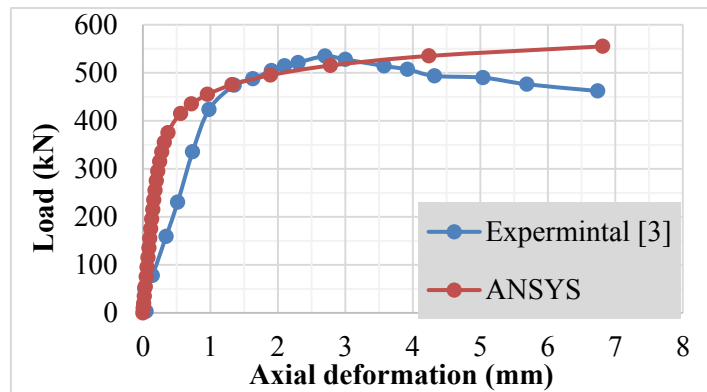


Figure (7): Experimental and numerical load-deflection behavior of circular CFT Square CFT

In Figure (8), the finite element mesh used with 6136 elements and the deformed shape of square CFT are shown. The variation of stresses were indicated in Figure (9). At the beginnings of loading, the results of analytical curve do not correlate well with experimental as shown in Figure (10); the finite element load deflection curve in the linear range are somewhat stiffer than the experimental plot. After about 450 kN to failure load, the plots show good agreement with slight increase in ANSYS curve deflection than the experimental ones. The ratio between experimental and FE failure load is 0.96.

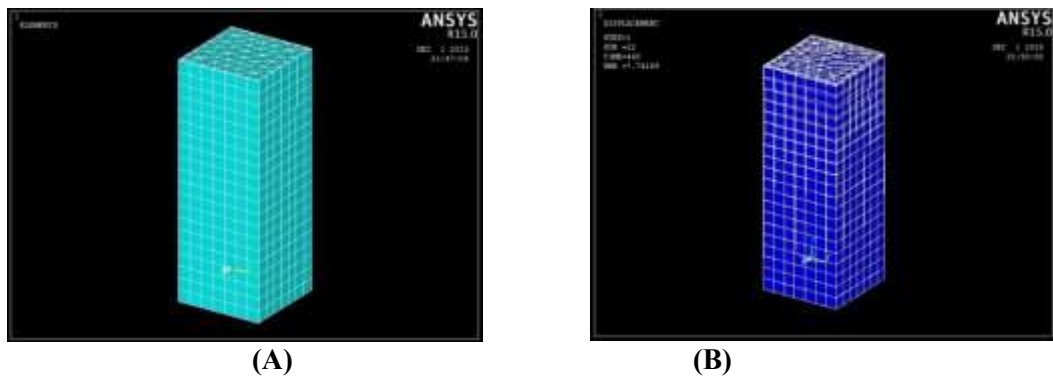


Figure (8): (A) Meshed model (B) Deformed shape

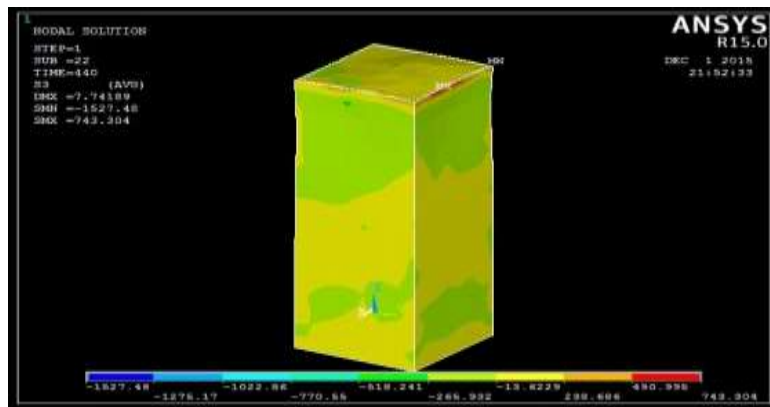


Figure (9): stresses variation of square CFT shape

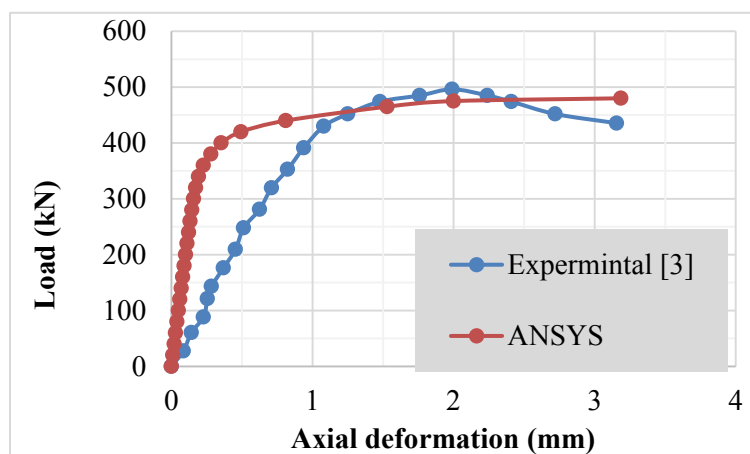


Figure (10): Experimental and numerical load-deflection behavior of square CFT

**Parametric study**

A parametric study has been performed for extra shapes of CFT by using finite element program ANSYS V.15. Finite element models are performed to determine the failure load for hexagonal and octagonal steel tubes shapes, and comparing the results with the previous ANSYS results for circular and square cross sections.

**Hexagonal CFT**

The materials properties for concrete and steel tube, meshing, loading, and boundary conditions are the same pattern used for circular CFT. A typical mesh for the hexagonal specimen with 5743 elements and the deformed shape are shown in Figure (11). The variation of stresses presented in Figure (12).

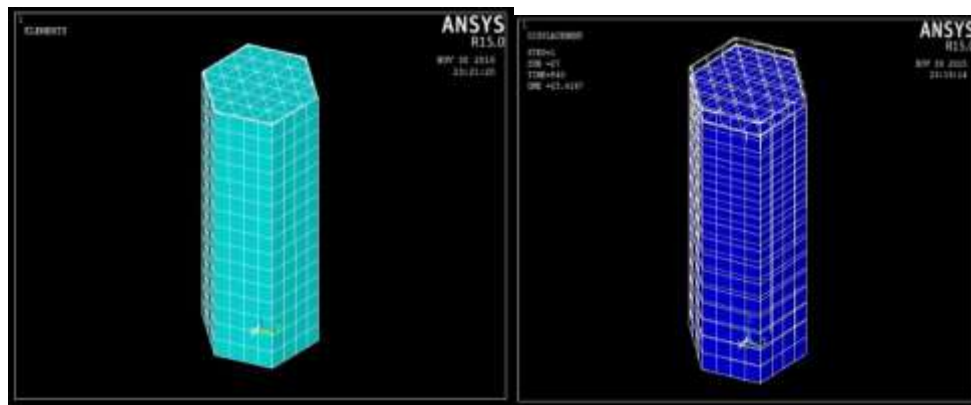


Figure (11): (A) Hexagonal CFT mesh made by ANSYS (B) Deformed shape

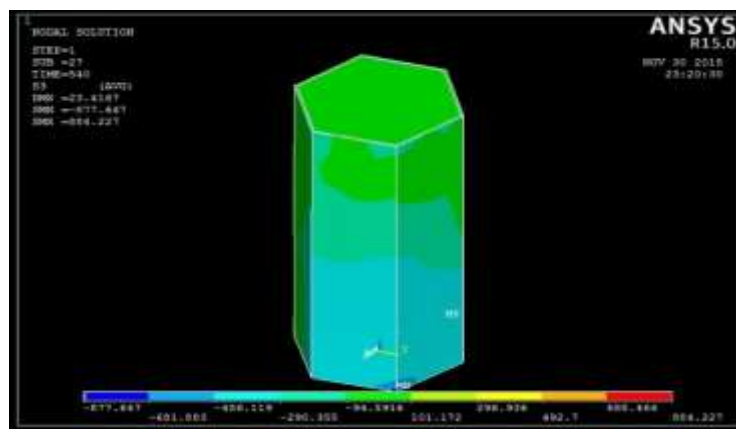


Figure (12): Stresses variation of Hexagonal CFT shape

**Octagonal CFT**

Volumes of steel tube and concrete core are created and meshed. The pattern of loading and boundary conditions are the same used for circular CFT. The overall mesh of the concrete and steel volumes with 1595 elements and deformed shape are shown in Figure (13). The variation of stresses presented in Figure (14).

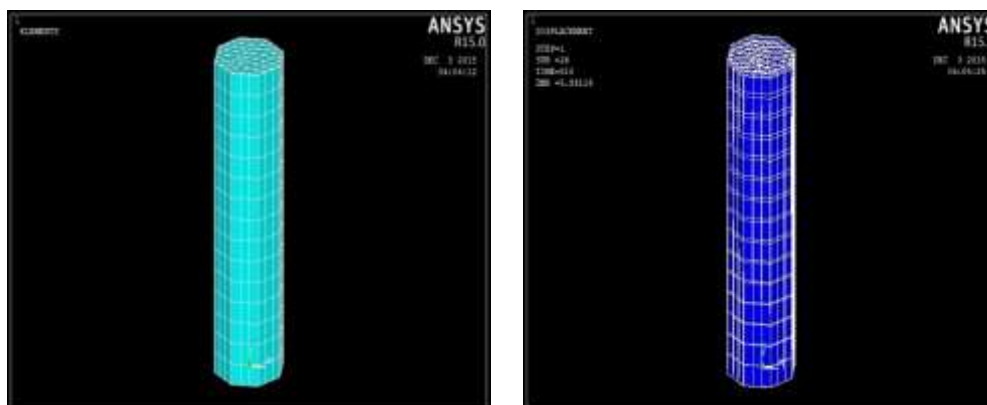


Figure (13): (A) Octagonal CFT mesh made by ANSYS (B) Deformed shape

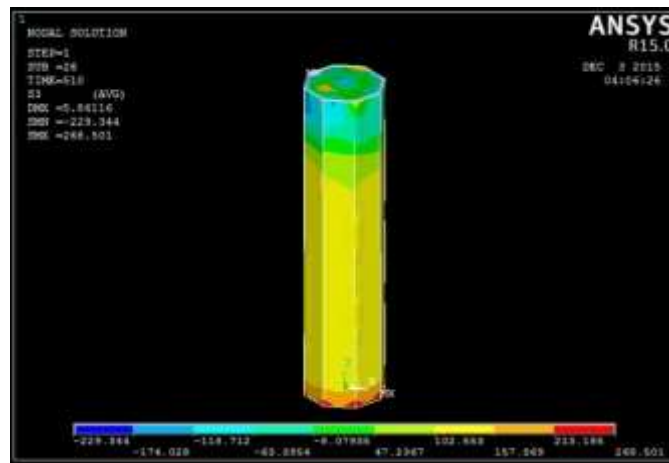


Figure (14): Stresses variation of octagonal CFT shape

In order to illustrate the finite element data for parametric results, the overall load-deflection curves obtained by using ANSYS for CFT columns are shown in Figure (15). By analyzing the load-deflection curves, it is possible to observe that the circular CFT has the highest failure load due to symmetrical confinement applied by circular steel tube which make the concrete core subjected to uniform three-dimensional compression, and that enhance the unit axial strength of concrete [10]. Although, the square CFT curve approximately has similar pattern to the circular cross section at linear part, but it has the lowest failure axial strength due to less confining action of square steel tube. The concrete core of square steel tube is divide to effective and non-effective confining zone. The effective confining zone, whose separated by quadratic parabola, increased by increasing the number of polygon sides approaching the circular shape as can be observed from the increasing in failure load of hexagonal and octagonal cross sections. In addition to less confinement of square steel tube, the local buckling appears due to the stress concentration at the corners. The ratio between finite element failure loads with respect to circular cross section is presented in Table (4).

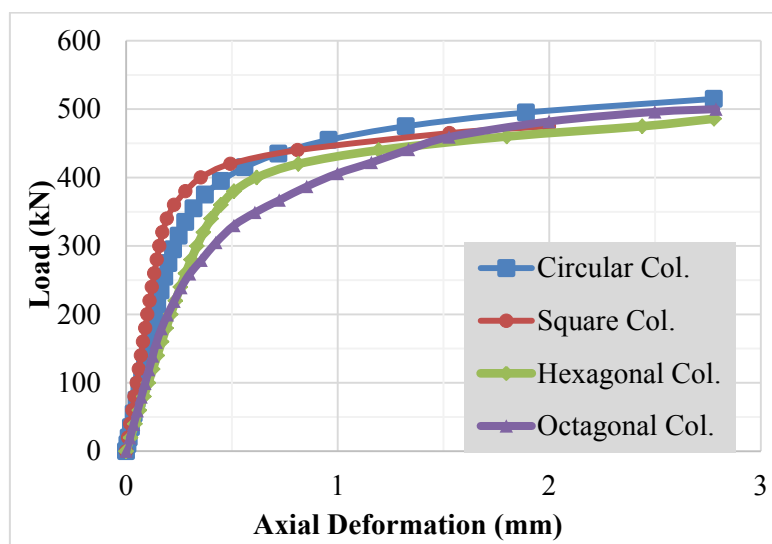


Figure (15): Overall numerical load-deflection behavior of CFT made by ANSYS

Table (4): Comparison between tested and ANSYS results

CFT columns	ANSYS load	Percentage ratio %
-------------	------------	--------------------

	(kN)	
Circular	515	---
Octagonal	500	0.97
Hexagonal	486	0.94
Square	475	0.92

### Analytical Study

#### 1- American Concrete Institute: Building code requirements for Structural Concrete (ACI 318- 14 Code) [7]:

ACI 318-14 code provision specifies the ultimate load for all composite columns (circular, square, rectangular, and polygon columns) by:

$$P_{ACI} = \phi P_n = 0.8 (0.85 A_c f_c + A_s f_y) \quad \dots (8)$$

Where:

$A_c$  and  $A_s$  are the areas of concrete core and steel tube respectively.

$f_c$  and  $f_y$  are the compressive strength of concrete and tensile strength of steel.

#### 2- Eurocode 2004 [11]:

The compression strength of composite columns is evaluated according to EC4 code as follows:

1. The ultimate axial force of a square column is:

$$P_{EC4} = A_c f_c + A_s f_y \quad \dots (9)$$

2. The ultimate axial force of a circular column (confinement effect takes into account if the relative slenderness  $\lambda$  is less than 0.5) where:

$$\lambda = \sqrt{\frac{(A_s f_y + 0.85 A_c f_c)}{N_{cr}}} \quad \dots (10)$$

$$N_{cr} = \frac{(E_s I_s + E_c I_c) \pi^2}{L^2} \quad \dots (11)$$

$$\eta_1 = 4.9 - 18.5 \lambda + 17 \lambda^2 + 1 \quad \dots (12)$$

$$\eta_2 = 0.25 (3 + 2 \lambda) \quad \dots (13)$$

$$P_{EC4} = A_s f_y \eta_2 + A_c f_c (1 + \eta_1 \frac{t f_y}{d f_c}) \quad \dots (14)$$

Where:

$N_{cr}$  is the elastic crippling load,  $E_c$  and  $E_s$  are the modulus of elasticity for concrete and steel,  $I_c$  and  $I_s$  are the moment of inertia for concrete and steel,  $\eta_1$  and  $\eta_2$  are coefficients,  $L$  is the length of column.

#### 3- AISC code [12]:

The load carrying capacity according to AISC Specifications is:

$$1- \text{ When } P_e \geq 0.44 P_0, P_n = P_0 [0.658^{(P_0/P_e)}] \quad \dots (15)$$

$$2- \text{ When } P_e < 0.44 P_0, P_n = 0.877 P_0 \quad \dots (16)$$

Where:

$P_0 = C_2 A_c F_c + A_s F_y$ , the value  $C_2$  is 0.85 for rectangular sections and 0.95 for circular sections.

$$P_e = \frac{\pi^2 E I_{eff}}{(L)^2}; E I_{eff} = E_s I_s + C_1 E_c I_c; C_1 = 0.6 + 2 \left( \frac{A_s}{A_c + A_s} \right) \leq 0.9$$

#### 4- New Zealand standard code [13]:

The axial strength of steel encased concrete sections according to NZ code is:

$$\phi_c P_{NZ} = C_2 A_c f_c + A_s f_y \quad \dots (17)$$

Where

$C_2 = 0.85$  for rectangular and 0.95 for circular composite sections;  $\phi_c = 0.75$ .

#### 5- Proposed method:

To obtain an accurate prediction of uniaxial compression strength of CFT, a proposed equation is formulated by using regression analysis in the following form:

$$P_{\text{Proposed}} = A_s f_y + 0.7 A_c^{0.8} f_{cc}^{0.95} \left( \frac{D \text{ or } B \text{ or } a}{t} \right)^{0.5} \quad \dots (18)$$

Where

B is the width of square CFT columns.

a is the side length of polygon CFT columns.

The proposed formulation is based on the following assumptions:

1. The confined strength of concrete (f<sub>cc</sub>) is used instead of compressive strength (f<sub>c'</sub>) with correction confinement coefficient representing by  $\left( \frac{D \text{ or } B \text{ or } a}{t} \right)^{0.5}$ .
2. Enhancements are added to the strength of concrete core contribution part.

This formula is validate by using 148 CFT experimental studies of solid circular [3, 4, 14-22], square [3, 4, 14, 15, 17-19, 23-25], rectangular [15-17], hexagonal and octagonal [26-28] columns. In Table (5), a comparison of convergent percentage (COV %) of CFT existing test columns based on (P test/ P cal.) ratio. The results indicate that the proposed equation (18) has the lowest COV percentage at 24.386% comparing with other methods.

**Table (5): comparison of predicted (P test/ P cal.) for 148 tested columns**

No	Methods	Mean	Standard deviation	COV %
1	ACI -318 Code	1.416	0.382	26.977
2	EC4 Code	0.975	0.246	25.230
3	AISC code	1.497	0.433	28.924
4	NZ Code	1.483	0.403	27.174
5	Eq. (18)	1.181	0.288	24.386

Figures (16) to (20) illustrate the relationship of (P test/ P cal.) for the design methods by ACI - 318M Code [7], EC4 Code [11], AISC code [12], NZ Code [13], and proposed equation (18). Among them, the axial strength based on the proposed formulae are the simply and closest to the experimental data. The results based on AISC design code are the most conservative.

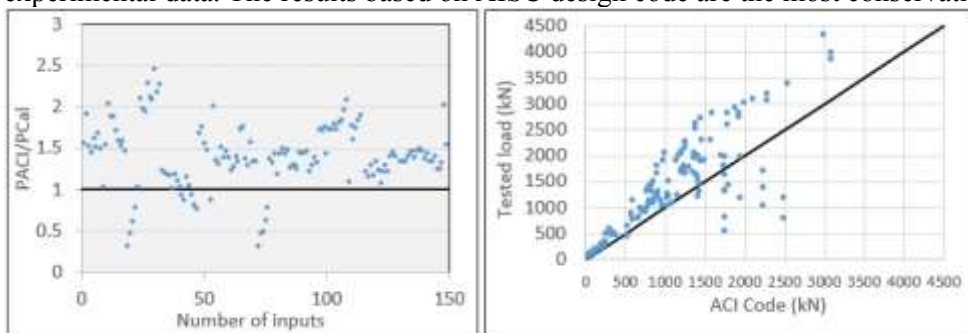


**Figure (16): ACI 318M-14 Code [7]**

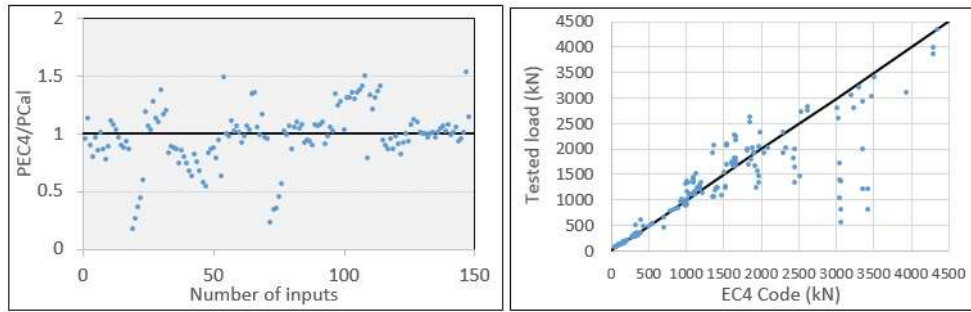


Figure (17): Eurocode 2004<sup>[11]</sup>

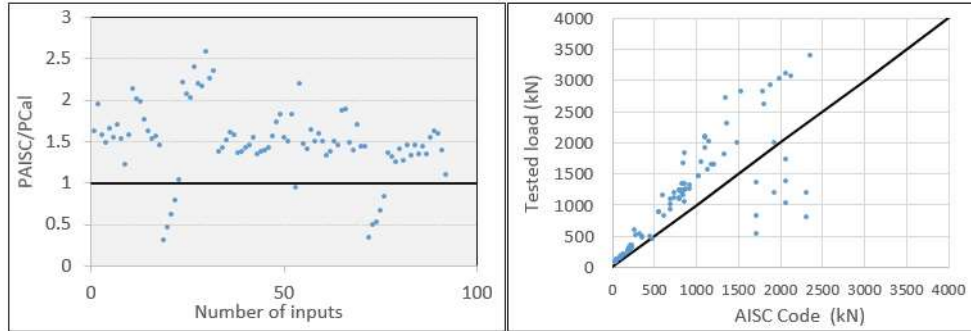


Figure (18): AISC Code 2010<sup>[12]</sup>

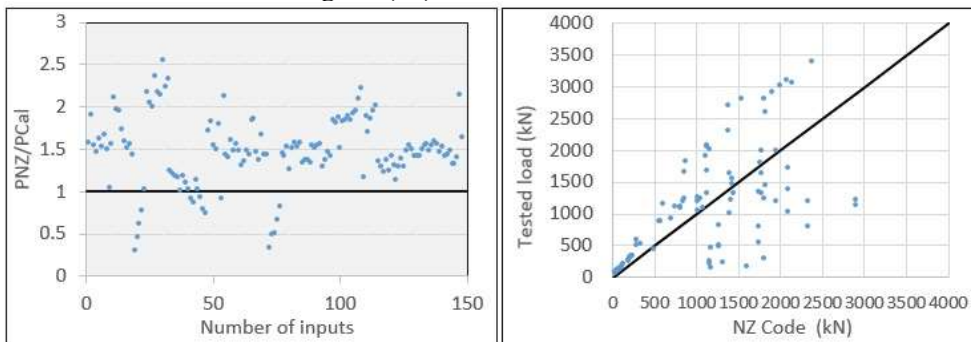


Figure (19): NZ Code 2006<sup>[13]</sup>

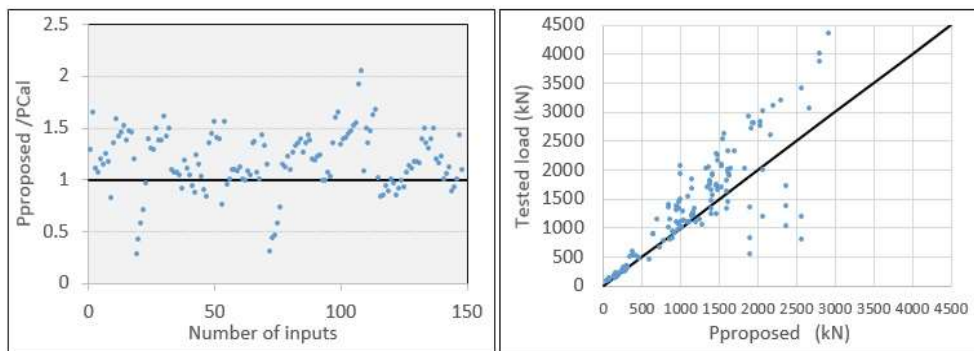


Figure (20): proposed equation (18)

Also, to check the validity of Equation (18), a comparison of ( $P_{ANSYS} / P_{Calculated}$ ) of CFT columns that previous analyzed by ANSYS as shown in Table (6).

Table (6): comparison of  $P_{ANSYS} / P_{Cal}$ .

CFT	ANSYS	$P_{ANSYS} / P_{Calculated}$
-----	-------	------------------------------

columns	Load (kN)	ACI %	EC4 %	AISC %	NZ %	By Eq. (18) %
Circular	515	1.77	0.93	1.81	1.80	1.38
Square	475	1.26	0.94	1.36	1.35	1.01
Hexagonal	486	1.54	1.14	1.09	1.64	1.08
Octagonal	500	2.01	1.53	1.39	2.14	1.42

**CONCLUSIONS**

CFT columns consist of a steel tube with a concrete core casted inside. The composite column may be of any shape; octagonal, square, circular, hexagonal, elliptical, etc. A finite element program ANSYS version 15 is used for modeling various cross-sections of composite columns. The comparison between ANSYS and experimental test results (for circular and square columns) were made to calibrate the correct representation of columns to simulate the other polygon cross section (hexagonal and octagonal). In general, the circular columns have highest failure load due to uniform confining effect compared with other shapes. Finally, a method to calculate the ultimate axial strength of CFT columns is proposed sections with side length ranging between 200 and 4000 mm. The prediction of the proposed method agreed well with large experimental data with simple form.

**REFERENCES:**

[1] Saadon A., Nasser K., and Mohamed I., “A Neural Network Model to Predict Ultimate Strength of Rectangular Concrete Filled Steel Tube Beam – Columns”, Engineering and Technology Journal, Volume 30, No.19, 2012.

[2] Ali A., Sadik S., and Abdul-Sahib W., "Strength and Ductility of Concrete Encased Composite Beams", Engineering and Technology Journal, Volume 30, No.15, 2012.

[3] Alwash N. A. and AL-Salih H. I., "Experimental investigation on behavior of SCC filled steel tubular stub columns strengthened with CFRP", Construction Engineering (CE), Volume 1 Issue 2, July 2013.

[4] Hu Hsuan-Teh, Huang Chiung-Shiann, Chen Zhi-Liang, "Finite element analysis of CFT columns subjected to an axial compressive force and bending moment in combination", Journal of Constructional Steel Research 61, 1692–1712, 2005.

[5] Richart F.E., Brandzaeg A., Brown R.L,” A study of the failure of concrete under combined compressive stresses”, Engineering Experimental Station/ University of Illinois, USA, 1928.

[6] Hu Hsuan-Teh, ASCE M., Huang C.S., Wu M. and Wu Y.,” Nonlinear analysis of axially loaded concrete-filled tube columns with confinement effect”, Journal of Constructional Steel Research, 2003.

[7] ACI 318M-14, American Concrete Institute, “Building Code Requirements for Structural Concrete,” American Concrete Institute, Farmington Hills, Michigan, September 2014.

[8] Mirmiran A., Zagers K. and Yuan W.,” Nonlinear finite element modeling of concrete confined by fiber composites”, Finite Elements in Analysis and Design, Elsevier science B.V., 2000.

[9] ANSYS, ANSYS User’s Manual Revision 15, ANSYS, Inc.

[10] Jian Cai and Zhen-Qiang He, "Axial load behavior of square CFT stub column with binding bars", Journal of Constructional Steel Research 62, pp. 472–483, September 2006.

[11] Eurocode 4: Design of Composite steel and concrete structures Part1-1: General rules and rules for buildings, EN 1994-1-1, 2004.

[12] AISC, Load and Resistance Factor Design Specifications for Structural Steel Building, American Institute of Steel Construction, Chicago, 2010.

[13] New Zealand Standard of concrete structures, “NZS 3101, Concrete Structures Standard”, 2006.

- [14] Baig M. N., Jiansheng F. and Jianguo N., "Strength of Concrete Filled Steel Tubular Columns, TSINGHUA science and technology, ISSN 1007-0214 05/15 pp. 657-666, Volume 11, Number 6, December 2006.
- [15] Bedage S.D and Shinde D.N, "Concrete filled steel tubes subjected to axial compression", IJRET: International Journal of Research in Engineering and Technology eISSN: 2319-1163 | pISSN: 2321-7308, Volume 4, Issue 6, June 2015.
- [16] Ghannam S., "Buckling of Concrete-Filled Steel Tubular Slender Columns", International Journal of Research in Civil Engineering, Architecture & Design, Volume 3, Issue 1, pp. 41-47, March 2015.
- [17] Jayalekshmi S. and Sankar Jegadesh J. S., "Finite element analysis and theoretical investigations on concrete filled steel tubular columns", proceeding of the international conference on Inter Disciplinary research in engineering and technology, 2014.
- [18] Schneider S. P., "axially loaded concrete-filled steel tubes", J. Structural Engineering, 124-10, 1125–1138, 1998.
- [19] Huang C., Yeh Y., Liu G., Hu H., Tsai K., Weng Y., Wang S. and Wu M., "Axial load behavior of stiffened concrete filled steel columns", J. Structural Engineering, 128-9, 1222–1230, 2002.
- [20] Khizer R. H., Narayana B.R. and Kumar N.S.," Numerical modelling of concrete composite steel tubes", International Journal of Research in Engineering and Technology, Volume 3, Special Issue 6, May 2014.
- [21] Zeghichea J. and Chaouib K.," An experimental behavior of concrete-filled steel tubular columns", Journal of Constructional Steel Research 61, pp. 53–66, 2005.
- [22] Laia M. and Hob J.," Uniaxial compression test of concrete filled steel tube columns confined by Tie Bars", 11th International Conference on Modern Building Materials, Structures and Techniques, 2013.
- [23] Liu D., "Tests on high-strength rectangular concrete-filled steel hollow section stub columns", Journal of Constructional Steel Research, 61(7):902-911, 2005.
- [24] Liu D. and Gho W., "Axial load behavior of high-strength rectangular concrete-filled steel tubular stub columns, [J].Thin-Walled Structures, 43(8):1131-1142, 2005.
- [25] Zhang S., Guo L., Ye Z. and Wang Y., "Behavior of steel tube and confined high strength concrete for concrete-filled RHS tubes", [J]. Advances in Structural Engineering, 8(2):101-116, 2005.
- [26] Zha X., "Hollow and solid concrete-filled steel tube structures", [M]. Beijing: Science Press, 2010.
- [27] Zhang Y., Wang Q., Mao X. and Cao B.," Research on mechanics behavior of stub-column of concrete-filled thin -walled steel tube under axial load, [J]. Building Structure, 35(1):22-27, 2005.
- [28] Tomii M., Yoshimura K., Morishita. Y.," Experimental studies on concrete-filled steel tubular stub columns under concentric loading", International Colloquium on Stability of Structures under Static and Dynamic Loads, Washington DC, 718-741, 1977.